Inorg. Chem. **2007**, *46*, 7097−7108

Alkylation and Acylation of Cyclotriphosphazenes

Mark A. Benson, Stefano Zacchini, Ramamoorthy Boomishankar, Yuri Chan, and Alexander Steiner*

Department of Chemistry, University of Liverpool, Crown Street, Liverpool L69 7ZD, U.K.

Received May 16, 2007

Phosphazenes $(RNH)_6P_3N_3$ (R = *n*-propyl, isobutyl, isopropyl, cyclohexyl, *tert*-butyl, benzyl) are readily alkylated at ring N sites by alkyl halides forming *N*-alkyl phosphazenium cations. Alkylation of two ring N sites occurred after prolonged heating in the presence of methyl iodide or immediately at room temperature with methyl triflate yielding *N*,*N*′-dimethyl phosphazenium dications. Geminal dichloro derivatives $Cl_2(RNH)_4P_3N_3$ are methylated by methyl iodide at the ring N site adjacent to both P centers carrying four RNH groups. X-ray crystal structures showed that the alkylation of ring N sites leads to substantial elongation of the associated P–N bonds. Both *N*-alkyl and *N*,*N*′-dialkyl phosphazenium salts form complex supramolecular networks in the solid state via NH···X interactions. Systems carrying less-bulky RNH groups show additional NH···N bonds between *N*-alkyl phosphazenium ions. *N*-Alkyl phosphazenium halides form complexes with silver ions upon treatment with silver nitrate. Depending on the steric demand of RNH substituents, either one or both of the vacant ring N sites engage in coordination to silver ions. Treatment of $(RNH)_6P_3N_3$ (R = isopropyl) with acetyl chloride and benzoyl chloride, respectively, yielded *N*-acyl phosphazenium ions. X-ray crystal structures revealed that elongation of P–N bonds adjacent to the acylated ring N site is more pronounced than it is in the case of N-alkylated species. Salts containing *N*-alkyl phosphazenium ions are stable toward water and other mild nucleophiles, while *N*,*N*′-dialkyl and *N*-acyl phosphazenium salts are readily hydrolyzed. The reaction of $(RNH)_6P_3N_3$ with bromoacetic acid led to N-alkylation at one ring N site in addition to formation of an amide via condensation of an adjacent RNH substituent with the carboxylic acid group. The resulting bromide salt contains mono cations of composition $(RNH)_5P_3N_3CH_2CONR$ in which a CH_2–C(O) unit is embedded between a ring N and an exocyclic N site of the phosphazene.

Introduction

Substitution reactions at P centers of poly- and cyclophosphazenes are well established and have led to a great variety of derivatives.[1] In contrast, the functionalization of the ring nitrogen centers has received far less attention apart from metal coordination.[2] The basicity of the phosphazene ring N centers is determined by the electronic properties of the substituents bound to neighboring phosphorus centers. Chloro phosphazenes are very weak bases (pKA ≈ −6) and require strong electrophiles to quaternize ring N sites, yielding labile products.[3] Organo- and organo amino-substituted phosphazenes are fairly basic (pKA ≈ 9) and are readily methylated in the presence of methyl iodide.[4] There is, however, scarce information on both the structural properties of the resultant *N*-methyl phosphazenium salts and the reactivity of cyclophosphazenes to organic electrophiles other than methyl iodide. We discovered that ring N-alkylation provides a convenient pathway toward polycationic systems consisting of phosphazene rings tethered together via ring N centers. We showed that 1,4-dibromobut-2-ene and α,α′-dibromo xylenes react with 2 equiv of cyclotriphosphazene,

* To whom correspondence should be addressed. E-mail: a.steiner@liv.ac.uk.

(1) (a) Chandrasekhar, V.; Krishnan, V. *Adv. Inorg. Chem.* **2002**, *53*, 159−211. (b) Allen, C. W. *Chem. Rev.* **1991**, *91*, 119−135. (c) Elias, A. J.; Shreeve, J. M. *Adv. Inorg. Chem.* **2001**, *52*, 335−358. (d) Mark, E. M.; Allcock, H. R.; West, R. *Inorganic Polymers*, 2nd Ed.; Oxford University Press: New York, 2005; pp 62−153. (e) Labarre, J. F. *Topics Curr. Chem.* **1985**, *129*, 173−260.

(2) (a) Steiner, A.; Zacchini, S.; Richards, P. I. *Coord. Chem. Rev.* **2002**, *227*, 193−216. (b) Chandrasekhar, V.; Nagendran, S. *Chem. Soc. Rev.* **2001**, *30*, 192−203. (c) Allcock, H. R.; Desorcie, J. L.; Riding, G. H. *Polyhedron* **1987**, *6*, 119−157. (d) Richards, P. I.; Benson, M. A.; Steiner, A. *Chem. Commun.* **2003**, 1392−1393. (e) Boomishankar, R.; Richards, P. I.; Steiner, A. *Angew. Chem., Int. Ed.* **2006**, *45*, 4632−4634. (f) Chandrasekhar, V.; Thilagar, P.; Murugesa Pandian, B. *Coord. Chem. Rev.* **2007**, *251*, 1045−1074.

(3) Zhang, Y.; Tham, F. S.; Reed, C. A. *Inorg. Chem.* **2006**, *45*, 10446−10448.

(4) (a) Allcock, H. R.; Levin, M. L.; Austin, P. E. *Inorg. Chem.* **1986**, *25*, 2281−2288. (b) Rapko, J. N.; Feistel, G. *Inorg. Chem.* **1970**, *9*, 1401−1405. (c) Searle, T. S.; Dyson, J.; Ranganathan, T. N.; Paddock, N. L. *J. Chem. Soc., Dalton Trans.* **1975**, 203−208. (d) Calhoun, H. P.; Trotter, J. *J. Chem. Soc., Dalton Trams.* **1974**, 377−381.

10.1021/ic7009463 CCC: $37.00
Published on Web 07/10/2007

Scheme 1. N-Alkylation Reactions

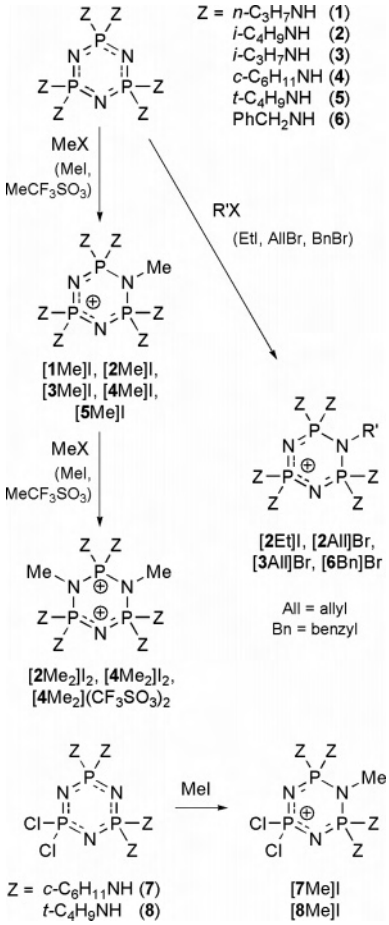

resulting in stable bromide salts. These contain dications in which a butenylene or xylylene unit links two phosphazene rings via ring N centers.[5] Here we report the syntheses and structures of a range of *N*-alkyl and *N*-acyl phosphazenium salts. These promise unusual properties and interesting applications in various areas, such as cationic surfactants, phase-transfer catalysts, ionic liquids, acyl transfer reagents, and supramolecular building blocks.

Results and Discussion

N-Alkylation. Syntheses. Cyclotriphosphazenes $(RNH)_6P_3N_3$ (R = *n*-propyl (**1**), isobutyl (**2**), isopropyl (**3**), cyclohexyl (**4**), *tert*-butyl (**5**))[6] were reacted with methyl iodide in either chloroform, THF, or toluene (see Scheme 1). Although methylation proceeds slowly at room temperature, refluxing the solutions gives complete conversion to *N*-methyl phosphazenium salts [**1**Me]I, [**2**Me]I, [**3**Me]I, [**4**Me]I, and [**5**Me]I within 24 h. The reactions were monitored using ^{31}P NMR spectroscopy. *N*-Methyl phosphazenium salts show AB_2 signals, which are shifted upfield compared to the singlet signals of the parent phosphazenes. After 48 h of refluxing, an additional AB_2 signal appears featuring a triplet at distinctly lower field, which indicated the formation of *N*,*N*′-dimethyl phosphazenium salts. The formation of [**2**Me$_2$]I$_2$ and [**4**Me$_2$]I$_2$ was complete after 72 h. The corresponding reaction with methyl triflate leads to complete conversion to [**4**Me$_2$](CF$_3$SO$_3$)$_2$ by stirring the reaction mixture at room temperature in chloroform for 20 min. It is noteworthy that further methylation did not occur even after prolonged heating in the presence of excess methyl triflate. *N*-Methyl phosphazenium salts are stable toward water, alcohols, and aqueous HCl. They degrade very slowly in methanol/KOH solution under formation of the parent phosphazenes. *N*,*N*′-Dimethyl phosphazenium salts are more reactive. They are cleaved by both water and alcohols, yielding the corresponding *N*-methyl phosphazenium derivatives.

Geminally substituted dichloro cyclotriphosphazenes $Cl_2(RNH)_4P_3N_3$ (R = cyclohexyl (**7**) and *tert*-butyl (**8**))[7] are regioselectively methylated by methyl iodide at the ring N site neighboring both P centers that carry RNH groups. Refluxing the reaction solutions for 24 h in either THF or toluene yielded [**7**Me]I and [**8**Me]I, respectively (Scheme 1). The regioselectivity of this reaction reflects the deactivating effect of chloro substituents at phosphorus.

The treatment of **2** with neat ethyl iodide at room temperature produced [**2**Et]I. However, reactions of higher alkyl halide homologues generated alkenes via β-elimination of monoprotonated phosphazenium iodides. Alkylation reactions using allyl bromide and benzyl bromide succeeded under reflux conditions, yielding [**2**All]Br, [**3**All]Br, and [**6**Bn]Br. Scheme 1 summarizes the reactions that yielded *N*-alkyl and *N*,*N*′-dialkyl phosphazenium salts. With the exception of [**6**Bn]Br, all compounds form colorless crystalline materials. [**6**Bn]Br, which features seven benzyl groups, exists as an oily liquid at room temperature that solidifies at −2 °C. It should be noted that *N*,*N*′-dialkylated products were not obtained even after prolonged refluxing of reaction mixtures containing an excess of allyl or benzyl bromide.

X-ray Crystallography. *N*-Alkyl derivatives crystallize with ease simply by evaporation of their methanol solutions. The crystallization of *N*,*N*′-dimethyl derivatives were carried out in aprotic solvents under inert gas atmosphere. With the exception of [**4**Me$_2$]I$_2$, all products listed in Scheme 1 have been structurally characterized by single-crystal X-ray diffraction. Solvates were obtained of [**4**Me]I·MeOH·H$_2$O, [**4**Me$_2$](CF$_3$SO$_3$)$_2$·CHCl$_3$, [**7**Me]I·CH$_3$I, and [**6**Bn]Br·2THF. Table 1 lists P−N bond lengths of *N*-methyl and *N*,*N*′-dimethyl phosphazenium ions. Topologically equivalent P−N bonds are very similar; thus, average values are given that are based on data obtained from good quality crystals of [**2**Me]I, [**4**Me]I·MeOH·H$_2$O and [**2**Me$_2$]I$_2$, [**4**Me$_2$](CF$_3$SO$_3$)$_2$·CHCl$_3$, respectively. In contrast to P−N bond lengths, the ring angles appear to be more flexible. For example, the P−N−P angles associated with the non-alkylated ring N atom measure 134.9° in [**4**Me$_2$](CF$_3$SO$_3$)$_2$·CHCl$_3$ and 127.4° in [**2**Me$_2$]I$_2$, while the other bonding parameters of the P$_3$N$_9$Me$_2$ cores of both structures are very similar. As a result,

(5) (a) Benson, M. A.; Steiner, A. *Chem. Commun.* **2005**, 5026−5028. (b) Benson, M. A.; Boomishankar, R.; Wright, D. S.; Steiner, A. *J. Organomet. Chem.* **2007**, *692*, 2768−2772.

(6) Bickley, J. F.; Bonar-Law, R.; Lawson, G. T.; Richards, P. I.; Rivals, F.; Steiner, A.; Zacchini, S. *Dalton Trans.* **2003**, 1235−1244.

(7) Chandrasekhar, V.; Vivekanandan, K.; Nagendran, S.; Senthil Andavan, G. T.; Weathers, N. R.; Yarbrough, J. C.; Cordes, A. W. *Inorg. Chem.* **1998**, *37*, 6192−6198.

Table 1. Average P−N Bond Lengths of *N*-Methyl (**A**) and *N*,*N*′-Dimethyl Phosphazenium Ions (**B**), [**2**Me]I, [**4**Me]I·MeOH·H_2O and [**2**Me_2]I_2, [**4**Me_2]$(CF_3SO_3)_2$·$CHCl_3$, Respectively

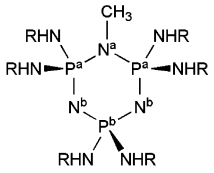

A

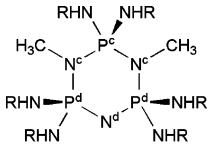

B

P^a-N^a	1.685	P^c-N^c	1.653
P^a-N^b	1.577	P^d-N^c	1.683
P^b-N^b	1.604	P^c-N^d	1.570
P^a-N^{exo}	1.624	P^c-N^{exo}	1.605
P^b-N^{exo}	1.646	P^d-N^{exo}	1.615
N^a-C	1.484	N^c-C	1.498
$\{\sum(P^a-N^j)\}/4$	1.627	$\{\sum(P^c-N^j)\}/4$	1.629
$\{\sum(P^b-N^j)\}/4$	1.625	$\{\sum(P^d-N^j)\}/4$	1.621

the P_3N_3 ring in [**4**Me_2]$(CF_3SO_3)_2$ is virtually planar while the sharper P−N−P angle in [**2**Me_2]I_2 causes its ring to pucker into a half-chair conformation.

The P−N(alkyl) bonds (P^a-N^a) in *N*-methyl phosphazenium ions **A** are on average 1.685 Å and are thus considerably longer than ring P−N bonds of the parent phosphazenes (1.60 Å).[6] These long bonds are neighbored by markedly shorter bonds (P^a-N^b, 1.577 Å), while the bonds furthest away from the alkylated N site (P^b-N^b, 1.604 Å) are comparable to ring P−N bonds of the parent systems. The *N*,*N*′-dimethyl phosphazenium ions **B** display long P−N bonds around methylated N sites, with P^d-N^c bonds (1.683 Å) being slightly longer than P^c-N^c bonds (1.653 Å). In contrast, the P−N bonds around the vacant site are rather short (P^d-N^d 1.570 Å). The exocyclic P−N bond lengths are also affected by N-alkylation, since they are shorter than in the parent phosphazenes where they amount to around 1.66 Å. The average P−N bond distance within each individual PN_4 tetrahedron ($D_i = \{\sum(P^i-N^j)\}/4$) is more or less constant for all the P centers listed in Table 1 ranging between 1.62 and 1.63 Å. This indicates that the elongation of P−N bonds due to alkylation is finely balanced by some distinct shortening of neighboring P−N bonds.[8]

The *N*-methyl and *N*,*N*′-dimethyl phosphazenium ions presented here are closely related to cyclodiphosphazanium ions $[\{(R_2N)_2PNR'\}_2]^{2+}$, **10**, which contain four-membered P_2N_2 rings featuring formal P−N single bonds.[9] In **10** there are two phosphonium centers that carry two amino substituents and are bridged by *N*-alkyl groups. The ring P−N bond lengths in **10** (av 168.4 Å) are similar to P−N(methyl) bond lengths observed in [**2**Me]I, [**4**Me]I·MeOH·H_2O and [**2**Me_2]I_2, [**4**Me_2]$(CF_3SO_3)_2$·$CHCl_3$. However, the chemistry of the four-membered ring system differs greatly from that of the six-membered ring systems presented here. While the latter cleave off alkyl groups under the formation of the parent cyclophosphazenes when treated with aqueous base, **10**

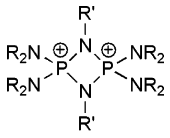

10

undergoes ring opening accompanied by P═O bond formation. This reflects the stability of six- over four-membered phosphazene rings. Accordingly, [**10**]Cl_2 is not obtained from alkylation of a cyclodiphosphazene, but via dimerization of phosphine imides $(R_2N)_2ClP{=}NR'$.

Recent theoretical studies on cyclophosphazenes suggest that there is a considerable amount of ionic contribution within the P−N ring bonds.[10] The notable bond elongation that the P−N ring bonds undergo upon alkylation and the similarity of resultant bond lengths with those found in **10** implies that the ionic contribution within the P−N(alkyl) bonds is reduced. The diagrammatic description given in Scheme 2 formally displays cationic tetravalent phosphonium centers, anionic divalent ring N centers, and neutral *N*-alkyl units.[2a] This representation correlates well with the variation of bond lengths discussed above. Ylidic P−N bonds (i.e., bonds between formally anionic divalent N centers and cationic tetravalent phosphonium centers, represented as dashed lines in **A**′ and **B**′) are short (∼1.57 Å) when the associated phosphonium centers are not engaged in further ylidic bonding (P^a-N^b in **A** and P^d-N^d in **B**). Slightly longer ylidic P−N bonds (∼1.60 Å) are observed when the associated phosphonium centers are involved in two ylidic bonds (P^b-N^b in **A** and also P−N(ring) bonds in parent phosphazenes).

Supramolecular Structures. The solid-state structures of all discussed compounds show extensive intermolecular networking via hydrogen bonding. This includes interionic NH···X bonds, NH···O bonds to solvent molecules, but also intercationic NH···N bonds. A variety of intermolecular NH···N contacts have been described for the parent phosphazenes $(RNH)_6P_3N_3$, which shows that the steric demand of NHR groups has a profound effect on the degree of networking in the solid state.[6] In the present study we were able to crystallize a series of solvate free *N*-alkyl phosphazenium iodides [**1**Me]I, [**2**Me]I, [**3**Me]I, and [**5**Me]I containing R groups of different steric demands. Their solid-state structures nicely demonstrate the effect that the R groups have on the number and type of hydrogen bonds. The *N*-alkyl phosphazenium ions in the *n*-propyl derivative [**1**Me]I are linked to two neighboring cations via pairs of NH···N bonds. This results in a polymeric chain of hydrogen-bonded cations. These chains are interlinked by iodide ions giving a 2D supramolecular arrangement (Figure 1). All six NH functions are engaged in hydrogen bonding. The isobutyl derivative [**2**Me]I contains dimers of *N*-alkyl phosphazenium ions linked by pairs of NH···N bonds. The dimers are joined in a 1D chain structure via iodide ions (Figure 2). Again, all

(8) See also: Bickley, J. F.; Copsey, M. C.; Jeffery, J. C.; Leedham, A. P.; Russell, C. A.; Stalke, D.; Steiner, A.; Stey, T.; Zacchini, S. *Dalton Trans.* **2004**, 989−995.

(9) (a) Thönnessen, H.; Jones, P. G.; Schmutzler, R. *Z. Anorg. Allg. Chem.* **2003**, *629*, 1265−1271. (b) Stahl, L. *Coord. Chem. Rev.* **2000**, *210*, 203−250.

(10) (a) Luana, V.; Pendas, A. M.; Costales, A.; Carriedo, G. A.; García-Alonso, F. J. *J. Phys. Chem. A* **2001**, *105*, 5280−5291. (b) Chaplin, A. B.; Harrison, J. A.; Dyson, P. J. *Inorg. Chem.* **2005**, *44*, 8407−8417.

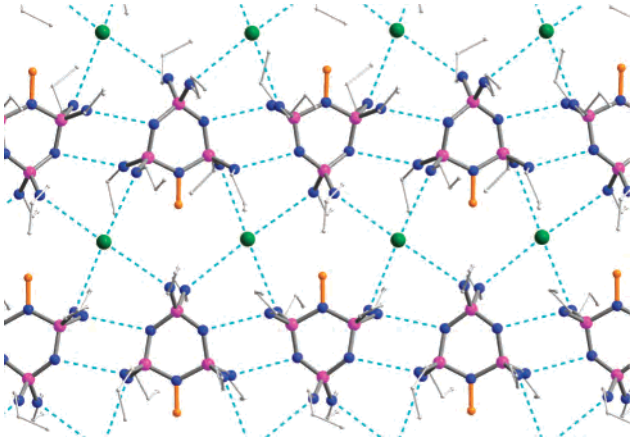

Figure 1. Supramolecular structure of [**1**Me]I. H atoms are omitted; hydrogen bonds are shown as dashed lines.

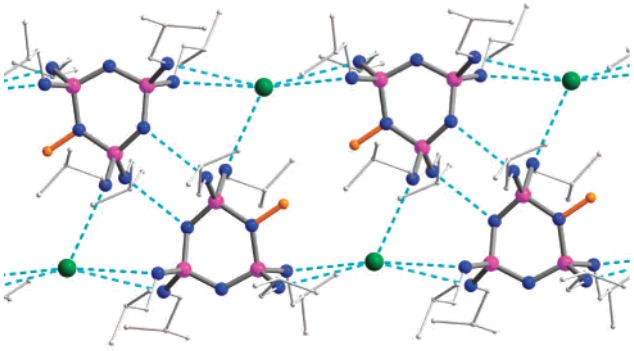

Figure 2. Supramolecular structure of [**2**Me]I. H atoms are omitted; hydrogen bonds are shown as dashed lines.

Scheme 2. Ylidic Representation of P−N Ring Bonds.

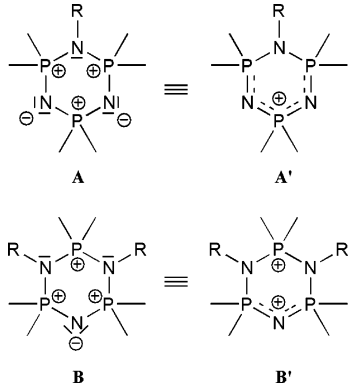

six NH groups are involved in hydrogen bonding. The isopropyl derivative [**3**Me]I does not form intercationic NH···N interactions, presumably due to the larger steric effect of R groups around potential H-bonding sites. Instead, the structure is connected solely through NH···I bonds resulting in a 2D supramolecular network (Figure 3), which features large H-bonded ring structures assembled from six ion pairs and smaller rings containing two ion pairs. Only five NH groups of the cation are taking part in H-bonding. Finally, the large bulk of *tert*-butyl groups in [**5**Me]I prevents both intercationic NH···N bonds and extensive networking. The supramolecular entity consists of two ion pairs that are linked via NH···I bonds (Figure 4). Here, only three NH functions of the cation are undergoing H-bonding. The cyclohexyl derivative [**4**Me]I crystallized as the solvate

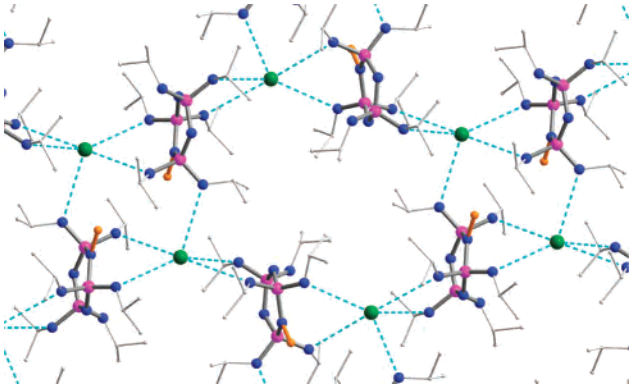

Figure 3. Supramolecular structure of [**3**Me]I. H atoms are omitted; hydrogen bonds are shown as dashed lines.

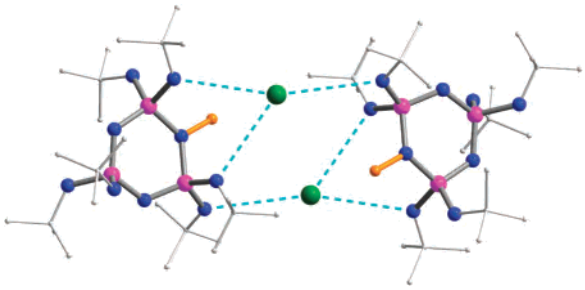

Figure 4. Supramolecular structure of [**5**Me]I. H atoms are omitted; hydrogen bonds are shown as dashed lines.

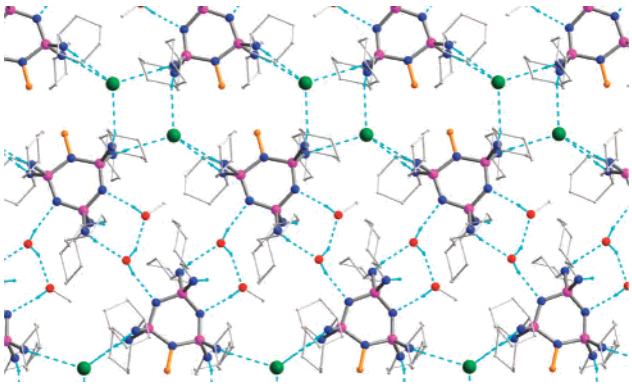

Figure 5. Supramolecular structure of [**4**Me]I·H_2O·MeOH. Hydrogen bonds are shown as dashed lines; oxygen atoms are displayed in red.

[**4**Me]I·MeOH·H_2O from methanol. The [**4**Me]$^+$ cations are linked via NH···I, NH···O, and OH···N(ring) bonds to form a complex two-dimensional network in the solid state (Figure 5).

The solid-state structure of the *N*,*N*′-dialkyl derivative [**2**Me_2]I_2 displays a 2D supramolecular structure. Intercationic NH···N interactions are absent most likely due to the higher charge of the system and the low acceptor properties of the vacant ring N site. All NH functions engage in H-bonding to iodide ions. There are two crystallographically unique iodide ions: One acts as a network node tying three cations together via NH···I bonds, while the other is bonded to solely one cation in a tridentate fashion via three NH···I bonds (Figure 6). In return, the NH functions can also be classified into two types. One is aligned equatorially (with respect to the P_3N_3 ring) and bonded to nodal iodide ions, while the other binds an iodide ion in tridentate fashion by

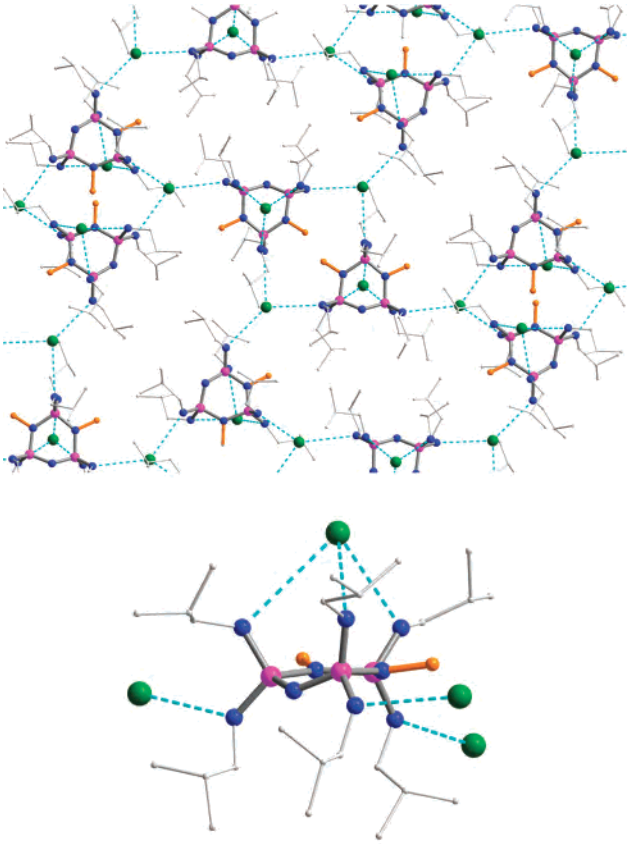

Figure 6. Supramolecular structure of $[\mathbf{2}Me_2]I_2$ (top) and side view of a $[\mathbf{2}Me_2]^{2+}$ ion showing its connectivity to iodide ions (bottom). H atoms are omitted; hydrogen bonds are shown as dashed lines.

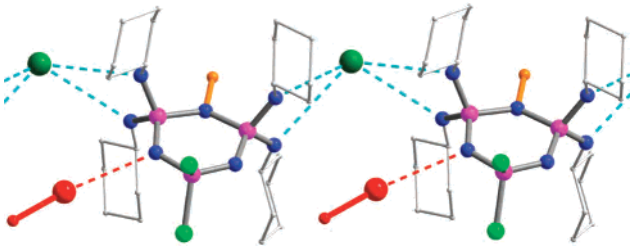

Figure 7. Supramolecular structure of [**7**Me]I·CH_3I. The methyl iodide molecule is shown in red, and its interaction with the ring N site is represented by the dashed red line.

pointing to an axial position. The network is assembled from rings containing four and two ion pairs, respectively.

[**7**Me]I crystallized as the solvate [7Me]I·CH_3I from a reaction solution containing excess methyl iodide. Phosphazenium cations are linked with iodide ions via NH···I bonds resulting in a supramolecular 1D aggregate (Figure 7). Again, all NH functions are involved in hydrogen bonding. Remarkably, the iodine atom of the methyl iodide molecule is in close contact with one of the vacant ring N sites. The N···I distance measures 3.359(3) Å, which is below the sum of the Van der Waals radii, and the C−I···N angle is nearly linear 163.9(1)°. Complexes of nitrogen heterocycles with organic iodides are not uncommon;[11] however, a complex with methyl iodide has not been

(11) See for example: Walsh, R. B.; Padgett, C. W.; Metrangolo, P.; Resnati, G.; Hanks, T. W.; Pennington, W. T. *Cryst. Growth Des.* **2001**, *2*, 165−175.

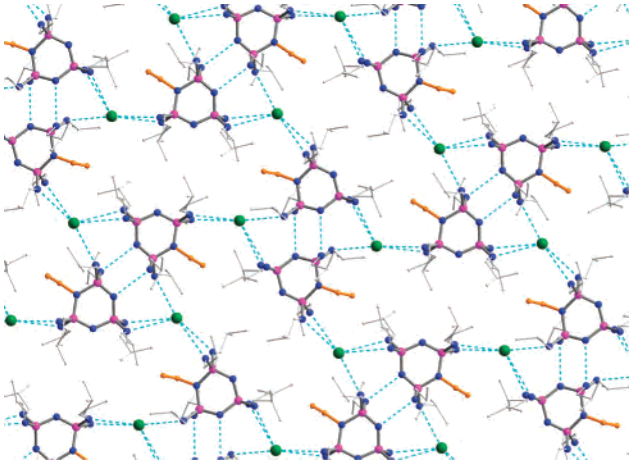

Figure 8. Supramolecular structure of [**2**Et]Br. H atoms are omitted; hydrogen bonds are shown as dashed lines.

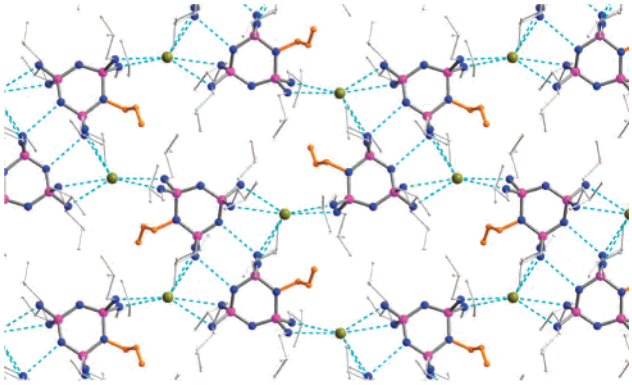

Figure 9. Supramolecular structure of [**2**All]Br. H atoms are omitted; hydrogen bonds are shown as dashed lines.

described so far. The *tert*-butyl derivative [**8**Me]I forms an aggregate analogous to that of [**5**Me]I in the solid state.

The crystal structures of [**2**Et]I (Figure 8) and [**2**All]Br (Figure 9) contain doubly NH···N bonded phosphazenium dimers, which are networked via bromide ions through NH···Br bonds. The doubly NH···N-bonded dimer motif was also observed in the solid-state structure of [**2**Me]I discussed above (see Figure 2) and seems to be a common motif for *N*-alkyl phosphazenium salts that are derived from the isobutyl derivative **2**. This demonstrates the strong structure-governing role of the alkyl amino side groups at the phosphazene. In addition, [**2**Me]I, [**2**Et]I, and [**2**All]Br share the same primary connectivity pattern: While one NH function is engaged in NH···N bonding, the other five bind to the halide ions in a way that every halide ion is connected to three phosphazenium ions, two of which are part of the same dimer. However, on a secondary level, there are several ways of 'hinging' the dimers around the halide ions and each structure completes the pattern differently. It should be added that the double NH···N bridge is a characteristic motif in

(12) (a) Rivals, F.; Steiner, A. *Z. Anorg. Allg. Chem.* **2003**, *629*, 139−146. (b) Bartlett, S. W.; Coles, S. J.; Davies, D. B.; Hursthouse, M. B.; Ibisogluc, H.; Kilic, A.; Shaw, R. A.; Ün, I. *Acta Crystallogr.* **2006**, *B62*, 321−329. The Cambridge Structural Database contained 54 structures featuring doubly NH···N bridged dimers of cyclotriphosphazenes.

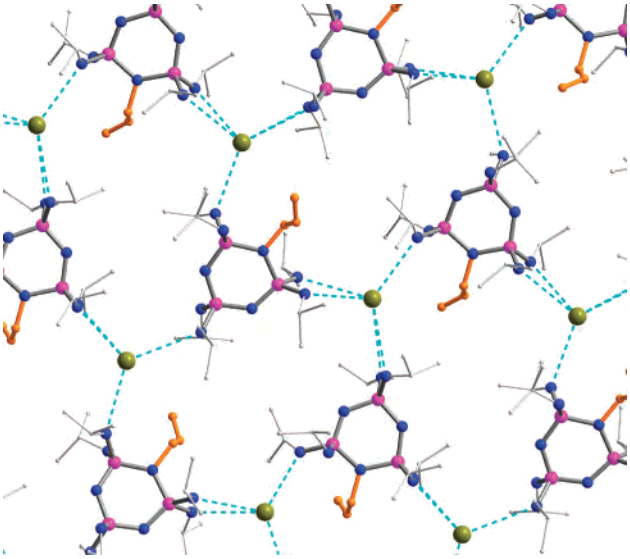

Figure 10. Supramolecular structure of [**3**All]Br. H atoms are omitted; hydrogen bonds are shown as dashed lines.

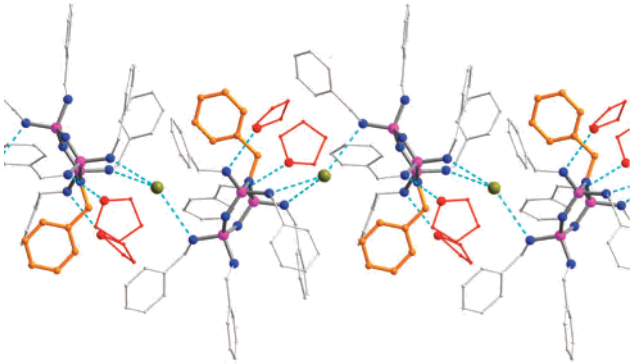

Figure 11. Supramolecular structure of [**6**Bn]Br·2THF. H atoms are omitted, hydrogen bonds are shown as dashed lines, and THF is displayed in red.

solid-state structures of cyclotriphosphazenes carrying RNH substituents.[6,12]

There is also some resemblance of the supramolecular structures of isopropyl derivatives [**3**All]Br and [**3**Me]I. Both structures form 2D networks via NH···halide bonds involving five NH groups per cationic unit and both lack the intercationic NH···N bonding. However, both systems are networked in a different way: In [**3**Me]I the iodide ions are chelated in a nongeminal fashion by NH groups of the same cation resulting in an orthogonal orientation of the P_3N_3 rings in relation to the network plane, while in [**3**All]Br the geminal chelation mode aligns P_3N_3 rings with the network plane (Figure 10).

As mentioned above, [**6**Bn]Br has a low melting point of −2 °C. It crystallizes from THF/hexane solution stored at −20 °C, forming the solvate [**6**Bn]Br·2THF. In the solid-state, this compound forms a 1D aggregate (Figure 11) in which the $[\mathbf{6}Bn]^+$ ions catenate with bromide ions via NH···Br bonds. In addition, each $[\mathbf{6}Bn]^+$ ion binds to two THF molecules via NH···O interactions. The resulting chains interact via a complex array of CH···π interactions between benzyl groups.

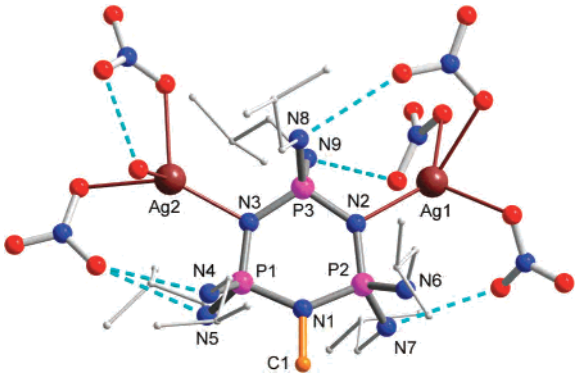

Figure 12. Crystal structure of $Ag_2[\mathbf{2}Me](NO_3)_3 \cdot H_2O$ showing the immediate coordination environment of Ag^+ ions. H atoms have been omitted. Dashed lines indicate hydrogen bonds. Selected bond lengths in Å: Ag1−N2 2.309(2), Ag2−N3 2.248(3), P1−N1 1.678(3), P1−N3 1.589-(3) P1−N4 1.623(3), P1−N5 1.613(3), P2−N1 1.675(3), P2−N2 1.587(3) ,P2−N6 1.609(3), P2−N7 1.621(3), P3−N2 1.610(3), P3−N3 1.614(3), P3−N8 1.634(3), P3−N9 1.615(3).

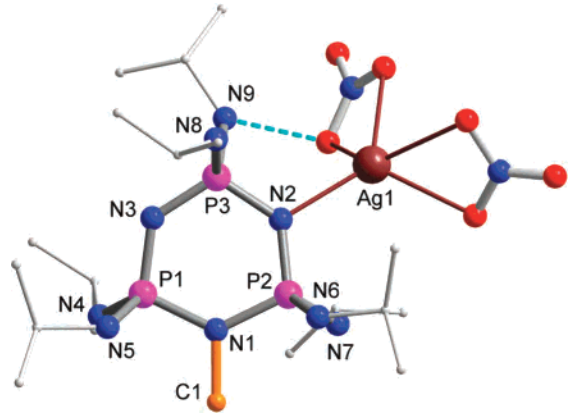

Figure 13. Crystal structure of $Ag[\mathbf{3}Me](NO_3)_2 \cdot MeOH$ showing the immediate coordination environment of Ag^+ ions. H atoms have been omitted. Dashed lines indicate hydrogen bonds. Selected bond lengths in Å: Ag1−N2 2.260(5), P1−N1 1.686(5), P1−N3 1.585(6), P1−N4 1.614-(5), P1−N5 1.614(6) P2−N1 1.665(5), P2−N2 1.591(5), P2−N6 1.609-(5), P2−N7 1.617(5), P3−N2 1.618(5), P3−N3 1.579(6), P3−N8 1.641(6), P3−N9 1.630(6).

Silver Complexes. Recently, we have shown that the parent phosphazenes $(RNH)_6P_3N_3$ are able to coordinate to Ag^+ ions via ring N sites, resulting in coordination polymers containing linear N−Ag−N linkages.[13] In order to probe the coordination potential of cationic *N*-methyl phosphazenium ions, we treated *N*-methyl phosphazenium iodides with excess silver nitrate in methanol. After filtration from the precipitated silver iodide, crystals were obtained of $Ag_2[\mathbf{2}Me](NO_3)_3 \cdot H_2O$, $Ag[\mathbf{3}Me](NO_3)_2 \cdot MeOH$, and $[\mathbf{5}Me]NO_3$, respectively. Evidently, the number of coordinated metal ions per ligand is governed by the steric effects of the R group. The low steric demand of the isobutyl group enables both vacant ring N sites of $[\mathbf{2}Me]^+$ (Figure 12) to coordinate to silver ions. In contrast, only one N site of the isopropyl

(13) Richards, P. I.; Steiner, A. *Inorg. Chem.* **2004**, *43*, 2810−2817.
(14) (a) Ragnarsson, U.; Grehn, L. *Acc. Chem. Res.* **1998**, *31*, 494−501. (b) Heinrich, M. R.; Klisa, H. S.; Mayr, H.; Steglich, W.; Zipse, H. *Angew. Chem., Int. Ed.* **2003**, *42*, 4826−4828. (c) Spivey, A. C.; Arseniyadis, S. *Angew. Chem., Int. Ed.* **2004**, *43*, 5436−5441. (d) Grondal, C. *Synlett* **2003**, *10*, 1568−1569. (e) France, S.; Guerin, D. J.; Miller, S. J.; Lectka, T. *Chem. Rev.* **2003**, *103*, 2985−3012.

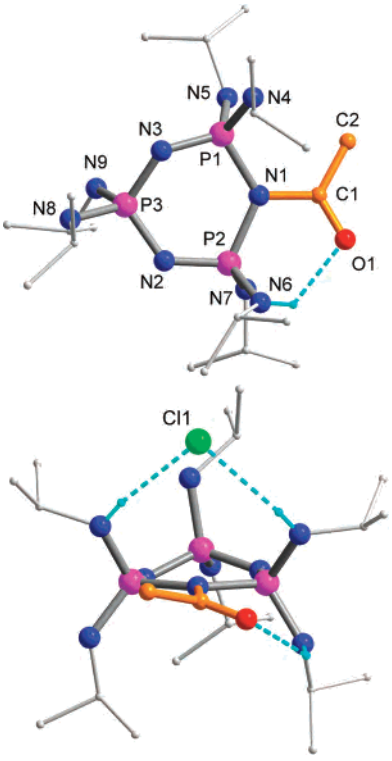

Figure 14. Two views of the crystal structure of [**3**Ac]Cl. H atoms have been omitted. Dashed lines indicate H-bonds. Selected bond lengths in Å: P1−N1 1.731(2), P2−N2 1.561(2), P1−N4 1.607(2), P1−N5 1.614(2), P2−N1 1.743(2), P2−N6 1.621(2), P2−N7 1.610(2), P3−N2 1.600(2), P3−N3 1.599(2), P3−N8 1.627(2), P3−N9 1.643(2), O1−C1 1.212(3), C1−N1 1.423(3), C1−C2 1.502(4).

derivative [**3**Me]$^+$ binds a metal ion (Figure 13), while the *tert*-butyl derivative [**5**Me]$^+$ does not coordinate at all but only undergoes ion exchange. In both Ag complexes, the silver ions are tetrahedrally coordinated by one ligand N site and three oxygen centers of nitrate ions. A water molecule completes the tetrahedral coordination geometry of one of the silver ions in Ag_2[**2**Me]$(NO_3)_3$·H_2O. The excess of nitrate ions might prevent the formation of linear N−Ag−N bridges between phosphazenium ions. In addition to metal coordination, both compounds are networked via extensive arrays of NH···O interactions. A comparison of P−N bond lengths of [**2**Me]I with those of both Ag complexes reveals that the coordination of phosphazenium cations to silver ions slightly lengthens the associated P−N bonds.

N-Acylation. Cyclophosphazenes $(RNH)_6P_3N_3$ readily react with acetyl and benzoyl chloride at room temperature in THF solution (see Scheme 3). ^{31}P NMR spectra of reaction mixtures containing a 1:1 ratio of reagents exhibit AB_2 signals. We were able to isolate *N*-acyl phosphazenium salts [**3**Ac]Cl and [**3**Bz]Cl and determine their crystal structures.

(15) In a typical experiment, a mixture of the secondary or tertiary alcohol (1 mol equiv), acetic anhydride (2 mol equiv), triethyl amine as auxiliary base (5 mol equiv), and the phosphazene (0.1 mol equiv) was stirred in chloroform. Reactions were monitored using TLC (ethyl acetate) against reaction mixtures containing DMAP as catalyst (0.1 mol equiv) and reaction mixtures containing no catalyst. While reactions with DMAP progressed, no reaction occurred in the presence of phosphazenes or the absence of a catalyst.

(16) Wagner, R.; Wiedel, B.; Günther, W.; Görls, H.; Anders, E. *Eur. J. Org. Chem.* **1999**, 2383−2390.

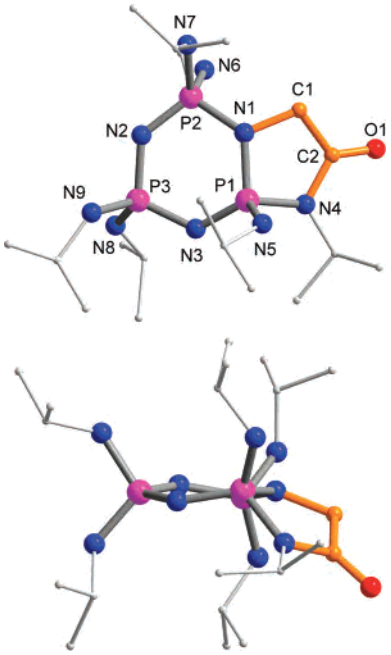

Figure 15. Crystal structure of **9** showing two views from different angles. H atoms and the bromide ion have been omitted. Selected bond lengths in Å: P1−N1 1.680(6), P1−N3 1.559(6), P1−N4 1.687(6), P1−N5 1.591-(6), P2−N1 1.690(6), P2−N2 1.553(6), P2−N6 1.615(6), P2−N7 1.621-(5), P3−N2 1.617(5), P3−N3 1.615(6), P3−N8 1.608(6), P3−N9 1.649(6), N1−C1 1.490(9), N4−C2 1.394(10), C1−C2 1.528(10), O1−C2 1.216(8).

Scheme 3. N-Acylation Reactions

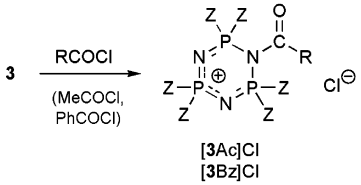

Scheme 4

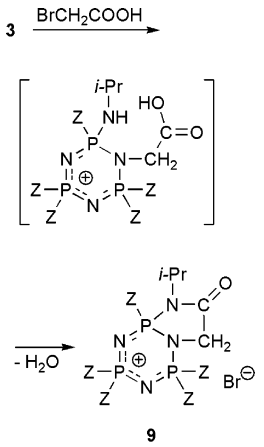

These confirmed that acylation occurred at one ring N site. Further addition of acyl chloride led to reaction mixtures that gave a complex signal pattern in ^{31}P NMR spectra. This suggests that reactions progress beyond the monoacylation stage. However, we were not able to isolate pure compounds from the resulting product mixtures.

Both [**3**Ac]Cl and [**3**Bz]Cl are moisture sensitive. In the presence of water, they readily produce acetic acid and benzoic acid, respectively. Preliminary tests show that *N*-acyl

Table 2. Crystallographic Data

compound	[**1**Me]I	[**2**Me]I	[**3**Me]I	[**4**Me]I·MeOH·H_2O	[**5**Me]I
chemical formula	$C_{19}H_{51}IN_9P_3$	$C_{25}H_{63}IN_9P_3$	$C_{19}H_{51}IN_9P_3$	$C_{38}H_{81}IN_9O_2P_3$	$C_{25}H_{63}IN_9P_3$
fw	625.50	709.65	625.50	915.93	709.65
cryst syst	monoclinic	triclinic	monoclinic	monoclinic	triclinic
space group	$P2_1/n$	$P\bar{1}$	$P2_1/n$	$C2/c$	$P\bar{1}$
a, Å	23.472(4)	11.484(1)	13.205(1)	29.374(2)	10.322(3)
b, Å	13.582(2)	12.838(1)	16.604(2)	11.0372(6)	11.793(3)
c, Å	38.636(6)	14.813(1)	14.607(2)	31.789(2)	16.481(4)
α, deg	90	94.308(2)	90	90	92.571(6)
β, deg	100.158(3)	108.880(2)	100.66(3)	115.646(1)	101.898(5)
γ, deg	90	111.935(2)	90	90	105.756(6)
V, Å^3	12124(3)	1868.6(3)	3147.4(6)	9290.9(9)	1878.4(8)
Z	16	2	4	8	2
μ(Mo Kα)/cm^{-1}	1.239	1.013	1.193	0.834	1.008
ρ(calcd)/g cm^{-1}	1.371	1.261	1.320	1.310	1.255
reflns, total	26 037	9511	11 913	23 545	6825
reflns, unique	7251	6383	4021	8171	6825
R_{int}	0.096	0.018	0.044	0.017	0.031
$2\theta_{max}$, deg	35	50	45	50	50
params	533	367	317	505	381
R1 ($F > 4\sigma(F)$)	0.090	0.040	0.062	0.026	0.034
wR2 (all data)	0.243	0.118	0.144	0.066	0.088

compound	[**2**Me_2]I_2	[**4**Me_2]$(CF_3SO_3)_2$·$CHCl_3$	[**7**Me]I·CH_3I	[**8**Me]I	[**2**Et]I
chemical formula	$C_{26}H_{66}I_2N_9P_3$	$C_{41}H_{79}Cl_3F_6N_9O_6P_3S_2$	$C_{26}H_{54}Cl_2I_2N_7P_3$	$C_{17}H_{43}Cl_2IN_7P_3$	$C_{26}H_{65}IN_9P_3$
fw	851.59	1171.51	882.37	636.29	723.68
cryst syst	monoclinic	monoclinic	triclinic	triclinic	monoclinic
space group	$P2_1/n$	$C2/c$	$P\bar{1}$	$P\bar{1}$	$P2_1/c$
a, Å	10.6808(5)	19.742(1)	10.4381(7)	9.0159(6)	12.184(2)
b, Å	18.1223(9)	16.8937(8)	11.1776(8)	11.4296(7)	16.000(2)
c, Å	21.499(1)	17.5708(8)	17.368(1)	14.554(1)	20.652(3)
α, deg	90	90	108.413(1)	92.961(1)	90
β, deg	103.539(1)	106.754(1)	95.749(1)	104.931(1)	101.41(2)
γ, deg	90	90	104.783(1)	100.017(1)	90
V, Å^3	4045.8(3)	5611.5(5)	1822.6(2)	1419.6(2)	3947(1)
Z	4	4	2	2	4
μ(Mo Kα)/cm^{-1}	1.701	0.394	2.032	1.504	0.960
ρ(calcd)/g cm^{-1}	1.398	1.387	1.608	1.489	1.218
reflns, total	20 867	14 492	9618	7426	20 651
reflns, unique	7104	4951	6330	4918	5050
R_{int}	0.060	0.019	0.019	0.020	0.128
$2\theta_{max}$, deg	50	50	50	50	45
params	395	335	363	296	334
R1 ($F > 4\sigma(F)$)	0.025	0.044	0.031	0.028	0.057
wR2 (all data)	0.051	0.113	0.076	0.076	0.157

compound	[**2**All]Br	[**3**All]Br	[**6**Bn]Br·2THF	Ag_2[**2**Me]$(NO_3)_3$·H_2O	Ag[**3**Me]$(NO_3)_2$·MeOH
chemical formula	$C_{27}H_{65}BrN_9P_3$	$C_{21}H_{53}BrN_9P_3$	$C_{57}H_{71}BrN_9O_2P_3$	$C_{25}H_{65}Ag_2N_{12}O_{10}P_3$	$C_{20}H_{55}AgN_{11}O_7P_3$
fw	688.70	604.54	1087.05	1002.54	762.53
cryst syst	monoclinic	orthorhombic	orthorhombic	monoclinic	monoclinic
space group	$P2_1/n$	$P2_12_12_1$	$P2_12_12_1$	$P2_1/n$	Cc
a, Å	15.407(2)	16.5652(9)	16.745(3)	9.1980(6)	17.958(2)
b, Å	14.853(2)	18.812(1)	18.004(5)	23.398(2)	17.781(2)
c, Å	16.932(2)	31.811(2)	19.026(3)	19.585(1)	11.706(1)
α, deg	90	90	90	90	90
β, deg	96.987(2)	90	90	94.365(1)	102.812(2)
γ, deg	90	90	90	90	90
V, Å^3	3845.9(8)	9913(1)	5736(2)	4202.6(5)	3644.9(6)
Z	4	12	4	4	4
μ(Mo Kα)/cm^{-1}	1.223	1.414	0.849	1.108	0.735
ρ(calcd)/g cm^{-1}	1.189	1.215	1.259	1.584	1.390
reflns, total	19 483	52 112	36 489	21 231	9262
reflns, unique	6773	17 436	9043	7381	4602
R_{int}	0.119	0.071	0.069	0.031	0.0289
$2\theta_{max}$, deg	50	50	48.5	50	50
params	374	617	659	478	381
R1 ($F > 4\sigma(F)$)	0.054	0.060	0.036	0.034	0.046
wR2 (all data)	0.145	0.145	0.068	0.077	0.119

compound	[**5**Me](NO_3)	[**3**Ac]Cl	[**3**Bz]Cl·$^1/_2$THF	**9**
chemical formula	$C_{25}H_{63}N_{10}O_3P_3$	$C_{20}H_{51}ClN_9OP_3$	$C_{27}H_{57}ClN_9O_{1.5}P_3$	$C_{20}H_{49}BrN_9OP_3$
fw	644.76	562.06	660.18	604.50
cryst syst	triclinic	tetragonal	monoclinic	monoclinic

Table 2. (Continued)

compound	[**5**Me](NO$_3$)	[**3**Ac]Cl	[**3**Bz]Cl·$^1/_2$THF	**9**
space group	$P\bar{1}$	$I\bar{4}$	$P2_1/n$	$P2_1/n$
a, Å	9.975(2)	19.0853(5)	14.000(1)	15.875(5)
b, Å	11.719(2)	19.0853(5)	15.090(1)	11.885(4)
c, Å	16.369(3)	17.4995(9)	17.905(2)	17.003(6)
α, deg	77.702(4)	90	90	90
β, deg	73.267(4)	90	109.135(2)	99.245(6)
γ, deg	74.620(4)	90	90	90
V, Å^3	1747.4(5)	6374.2(4)	3573.7(6)	3166(2)
Z	2	8	4	4
μ(Mo Kα)/cm^{-1}	0.212	0.299	0.277	1.478
ρ(calcd)/g cm^{-1}	1.225	1.171	1.227	1.268
reflns, total	4644	16 724	14 469	12 117
reflns, unique	4644	5600	4625	4078
R_{int}	−	0.036	0.064	0.128
$2\theta_{max}$, deg	45	50	45	45
params	390	350	402	319
R1 ($F > 4\sigma(F)$)	0.055	0.034	0.038	0.069
wR2 (all data)	0.137	0.085	0.061	0.158

phosphazenium salts react with alcohols under formation of esters. This promises useful applications for phosphazenes as acyl-transfer reagents, as well as nucleophilic catalysts for esterification of tertiary and secondary alcohols.[14] In view of the excellent catalytic performance of electron-rich pyridine derivatives such as DMAP (4-dimethylamino pyridine), we have studied the catalytic activity of electron-rich phosphazenes $(RNH)_6P_3N_3$ in the esterification of alcohols with acetic anhydride. However, our tests revealed that phosphazenes did not exhibit any catalytic effect in these reactions.[15] ^{31}P NMR experiments showed that phosphazenes form labile complexes with acetic anhydride, which are, presumably, too stable to react with bulkier alcohols. In contrast, acyl pyridinium cations have been reported to be very labile and highly reactive.[16] The crystal structures of [**3**Ac]Cl and [**3**Bz]Cl show that NHR groups adjacent to the acylated N site exhibit steric bulk around the electrophilic C(acyl) atom. This would have an impeding effect on an approaching nucleophile. Both structures reveal other interesting features. The acyl groups form intramolecular NH···O contacts with neighboring RNH groups (Figure 14). As a result, the mean planes of the O═C−R units of acyl groups are slightly twisted along the N−C(aryl) bond with respect to the adjacent P−N−P units of the phosphazene rings (17.0° in [**3**Ac]Cl, 25.3° in [**3**Bz]Cl). The elongation of P−N bonds adjacent to the *N*-acyl center is even more pronounced than in the *N*-alkyl derivatives. The average P−N(acyl) bond length in [**3**Ac]Cl and [**3**Bz]Cl amounts to 1.74 Å, which is considerably longer than the P−N(alkyl) bonds (see above). In return, the associated N−C bonds are shorter (av 1.42 Å) than in the *N*-alkyl derivatives. This demonstrates the electron-withdrawing power of the acyl group, which drains electron density away from the N center and reduces the ionic contribution within the two associated P−N bonds. The chloride ions in both structures bind to two RNH groups adjacent to the *N*-acyl unit via NH···Cl bonds. This ion-pairing motif puts the chloride ions right above the N−C(acyl) bond. If this arrangement is sustained in solution, it may also contribute to the shielding of the electrophilic C(acyl) centers.

Reaction with Bromoacetic Acid. With the aim of generating zwitterionic species reminiscent of α-amino acids, we reacted **3** with bromoacetic acid in THF under reflux conditions. The ^{31}P NMR spectrum of the resultant solution indicated the presence of two products in a 7:3 ratio based on signal integrals: The major product shows a singlet at 10.0 ppm, which can be attributed to the formation of [**3**H]$^+$ ions, while the minor product gave an ABC pattern, suggesting three chemically inequivalent phosphorus centers within the phosphazene ring. Single crystals of the minor product formed from a THF/hexane solution among the precipitate of the major species. It proved impossible to obtain a pure product; hence, spectroscopic data were generated from the mixture. The X-ray structure determination of the minor compound revealed the formation of the bicyclic compound **9** (Figure 15). In addition to alkylation at a ring N site, the carboxylic acid underwent condensation with a neighboring RNH group to form a cyclic amide. The resulting bromide salt contains mono cations of composition $(RNH)_5P_3N_3CH_2CONR$ in which a CH_2−C(O) unit is embedded between a ring N and an exocyclic N site of the phosphazene. It should be noted that no condensation reaction occurred when **3** was reacted with acetic acid instead of bromoacetic acid. Hence, we assume that alkylation of the ring N site is the first step in this reaction, which brings RNH and COOH groups into sufficiently close contact to undergo condensation (Scheme 4). In the presence of base (aqueous KOH) the organic moiety is cleaved on forming the parent phosphazene **3**.

The X-ray structure of **9** reveals that the bicyclic arrangement is strained. This is reflected by the rather sharp endocyclic N1−P1−N4 angle of 93.0(3)°. Likewise, the endocylic P1−N1−C1 angle is considerably sharper (110.5(4)°) than the corresponding exocylic P2−N1−C1 angle (117.5(5)°). The alkylated site N1 shows a pyramidally distorted environment with an angle sum of 354°. The P1−N4 bond which is associated with the amide N site is rather long when compared to other exocylic P−N bonds due to the electron-withdrawing effect of the adjacent carbonyl

group. The P−N bonds of the phosphazene ring in **9** are comparable to that of the *N*-methyl species discussed above.

Conclusion

We have shown that phosphazenes carrying organo amino side groups are readily alkylated at ring N sites by alkyl halides forming *N*-alkyl phosphazenium cations. Alkylation of two ring N sites succeeds after prolonged heating in the presence of methyl iodide or instantly at room temperature using methyl triflate yielding *N*,*N*′-dimethyl phosphazenium dications. X-ray crystal structures revealed that the alkylation of ring N sites leads to substantial elongation of the associated P−N bonds. We have attributed this to a decrease in electrostatic interaction within the polar phosphazene bonds. The great stability of *N*-alkyl phosphazenium cations, their ability to engage in complex supramolecular networking, their potential to undergo metal coordination, and the option of fine-tuning their steric properties promise interesting applications in various areas currently associated with organic cations.

This study also revealed that phosphazenes smoothly undergo N-acylation in the presence of acyl chlorides, forming stable *N*-acyl phosphazenium salts. The resulting products are readily cleaved by alcohols, which promises interesting uses as acyl transfer reagents or protecting groups in organic synthesis. Again, the option to modify NHR groups facilitates fine-tuning of steric and electronic properties and also the introduction of chiral side groups in close proximity to the reactive center. The bicyclic compound **9** obtained from the reaction of $(RNH)_6P_3N_3$ with bromoacetic acid showed that, in addition to N-alkylation, the neighboring exocyclic NHR groups can undergo condensation with carboxylic acid groups to form cyclic amides. This offers, in principle, interesting applications of phosphazenes as molecular platforms for the transformation of organic substrates.

Experimental Section

General Procedures. With the exception of the workup and crystallization of *N*-alkyl phosphazenium salts and the syntheses of silver complexes, all experiments were performed under inert gas atmosphere using standard Schlenk glassware. Solvents were dried using standard methods. Methanol was used as supplied. Phosphazenes were prepared as described previously.[6] Alkyl and acyl halides were distilled prior of use. FT-IR spectra were recorded on a Perkin-Elmer Paragon 1000 spectrometer in Nujol between CsI plates. NMR spectra were recorded from $CDCl_3$ solutions on a Bruker AMX 400 spectrometer at room temperature using $SiMe_4$ (for ^1H and ^{13}C) and 85% H_3PO_4 (for ^{31}P) as external standards (^1H NMR, 400.13 MHz; $^{13}C\{^1H\}$ NMR, 100.62 MHz; $^{31}P\{^1H\}$ NMR, 161.97 MHz).

***N*-Methyl Phosphazenium Iodides, [(RNH)$_6$P$_3$N$_3$Me]I.** [$(RNH)_6P_3N_3$Me]I were prepared by refluxing a mixture of $(RNH)_6P_3N_3$ (0.50 g) and excess methyl iodide (>2 mol equiv) in 20 mL of either chloroform, THF, or toluene for 24 h. The reaction progress was monitored with ^{31}P NMR. Alternatively, the reactions can be carried out in neat methyl iodide. Subsequently, all volatiles were removed in vacuum. Colorless crystals were obtained by slow evaporation of methanol solutions. [**1**Me]I: Yield 86%. mp: 128 °C. ^1H NMR: 0.92 (t, 18H, CH_3, $^3J_{HH}$ = 7.4 Hz), 1.57 (m, 12H, CH_2), 2.86 (m, 12H, NCH_2), 2.98 (t, 3H, NCH_3, $^3J_{HP}$ = 9.5 Hz), 3.90 ppm (br, 6H, NH). $^{13}C\{^1H\}$ NMR: 11.4, 24.8, 42.8, 47.0 ppm. $^{31}P\{^1H\}$ NMR: 17.5 (t), 19.2 ppm (d, $^2J_{PP}$ = 42.3 Hz). IR ν(cm^{-1}): 3178 (N−H), 1246, 1204, 1118 (P−N_{ring}), 1074 (P−N_{ring}), 1021, 895, 854, 791, 739. Anal. Calcd for $C_{19}H_{51}IN_9P_3$ (625.25): C, 36.48; H, 8.22; N, 20.13. Found C, 35.94; H, 7.97; N, 19.57%. [**2**Me]I: Yield: 89%. mp: 259−261 °C. ^1H NMR: 0.93 (m, 36H, CH_3), 1.78 (m, 6H, CH), 2.70 (m, 12H, CH_2), 2.95 (t, 3H, NCH_3, $^3J_{HP}$ = 9.6 Hz), 4.01 ppm (br, 6H, NH). $^{13}C\{^1H\}$ NMR: 20.2, 29.7, 48.6, 54.4 ppm. $^{31}P\{^1H\}$ NMR: 14.5 (t), 16.6 ppm (d, $^2J_{PP}$ = 43.8 Hz). IR ν(cm^{-1}): 3239 (N−H), 1261, 1224, 1197, 1128 (P−N_{ring}), 1090 (P−N_{ring}), 898, 823, 783, 759, 722. Anal. Calcd for $C_{25}H_{63}IN_9P_3$ (709.66): C, 42.31; H, 8.95; N, 17.76. Found C, 41.09; H, 8.73; N, 16.99%. [**3**Me]I: Yield 92%. mp: 164−165 °C. ^1H NMR: 1.12 (s, 36H, CH_3), 2.91 (t, 3H, $N_{ring}CH_3$, $^3J_{HP}$ = 9.6 Hz), 3.36 (m, 6H, CH), 3.65 ppm (m, 6H, NH). $^{13}C\{^1H\}$ NMR: 24.4, 42.4, 43.0. $^{31}P\{^1H\}$ NMR: 12.50 (t), 14.25 ppm (d, $^2J_{PP}$ = 43.7 Hz). IR ν(cm^{-1}): 3201 (N−H), 1267, 1219, 1164 (P−N_{ring}), 1135 (P−N_{ring}), 1061, 909, 859, 809, 722. Anal. Calcd for $C_{19}H_{51}IN_9P_3$ (625.50): C, 36.48; H, 8.22; N, 20.15. Found C, 36.25; H, 8.25; N, 19.90%. [**4**Me]I·MeOH·H_2O: Yield 88%. mp 295−297 °C. ^1H NMR: 1.12−1.93 (m, 60H, CH_2), 2.21 (m, 6H, CH), 2.97 (t, 3H, NCH_3, $^3J_{HP}$ = 9.4 Hz) 3.71 ppm (m, 6H, NH). $^{13}C\{^1H\}$ NMR: 25.5, 36.0, 36.4, 51.4, 58.8 ppm. $^{31}P\{^1H\}$ NMR: 12.42 (t), 15.52 ppm (d, $^2J_{PP}$ = 41.6 Hz). IR ν(cm^{-1}): 3201 (N−H), 1295, 1251, 1210, 1143 (P−N_{ring}), 1106 (P−N_{ring}), 1005, 903, 886, 848, 804, 784, 753, 722. Anal. Calcd for $C_{38}H_{75}IN_9OP_3$ (893.90): C, 51.06; H, 8.46; N, 14.10. Found C, 51.05; H, 8.81; N, 14.54%. [**5**Me]I: Yield 68%. mp: 200−201 °C. ^1H NMR: 1.37 (s, 54H, CH_3), 3.14 (t, 3H, NCH_3, $^3J_{HP}$ = 9.4 Hz), 3.70 ppm (br, 6H, NH). $^{13}C\{^1H\}$ NMR: 31.6, 52.4, 54.7 ppm. $^{31}P\{^1H\}$ NMR: 5.83 (t), 8.64 ppm (d, $^2J_{PP}$ = 43.6 Hz). IR ν(cm^{-1}): 3197 (N−H), 1265, 1224, 1157 (P−N_{ring}), 1028 (P−N_{ring}), 910, 884, 806, 739, 722. Anal. Calcd for $C_{25}H_{63}IN_9P_3$ (709.66): C, 42.31; H, 8.95; N, 17.76. Found C, 41.37; H, 8.92; N, 17.23%.

***N*,*N*′-Dimethyl Phosphazenium Diiodides, [(RNH)$_6$P$_3$N$_3$Me$_2$]I$_2$.** [$(RNH)_6P_3N_3Me_2$]I_2 were prepared by refluxing a mixture of $(RNH)_6P_3N_3$ (0.50 g) and excess methyl iodide (>3 mol equiv) in 20 mL of chloroform for 5 days. The reaction progress was monitored using ^{31}P NMR. Subsequently, all volatiles were removed in vacuum. Colorless crystals were obtained from chloroform solutions. [**2**Me_2]I_2: Yield 80%. mp: 179−182 °C. ^1H NMR: 0.84−0.96 (m, 36H, CH_3), 1.79 (m, 6H, CH), 2.77 (m, 12H, CH_2), 6.92 (m, 6H, NCH_3, $^3J_{HP}$ = 9.6 Hz), 4.36 ppm (br, 6H, NH). $^{13}C\{^1H\}$ NMR: 19.2, 28.6, 47.8, 48.9 ppm. $^{31}P\{^1H\}$ NMR: 13.19 (d), 33.00 ppm (t, $^2J_{PP}$ = 26.8 Hz). IR ν(cm^{-1}): 3164 (N−H), 1261, 1220, 1108 (P−N_{ring}), 1039 (P−N_{ring}) 967, 920, 901, 861, 818, 784, 741, 706, 624. Anal. Calcd for $C_{26}H_{66}I_2N_9P_3$ (851.59): C, 36.66; H, 7.76; N, 14.81. Found C, 37.80; H, 8.13; N, 14.37%. [**4**Me_2]I_2: Yield 89%. mp: 211−213 °C. ^1H NMR: 1.13−1.25 (m, 36H, CH_3), 1.90 (m, 6H, CH), 3.06 (m, 12H, CH_2), 4.28 (br, 6H, NH), 6.11 ppm (t, 6H, NCH_3, $^3J_{HP}$ = 10.6 Hz). $^{13}C\{^1H\}$ NMR: 23.9, 24.6, 34.4, 50.9 ppm. $^{31}P\{^1H\}$ NMR: 7.0 (d), 24.5 ppm (t, $^2J_{PP}$ = 32.7 Hz). IR ν(cm^{-1}): 3193 (N−H), 1298, 1282, 1263, 1108 (P−N_{ring}), 1033 (P−N_{ring}), 959, 938, 890, 846, 802, 722. Anal. Calcd for $C_{38}H_{78}I_2N_9P_3$ (1007.83): C, 45.29; H, 7.80; N, 12.51. Found C, 45.03; H, 7.87; N, 12.10%.

[4Me$_2$](CF$_3$SO$_3$)$_2$. Methyl triflate (0.40 mL, 3 equiv) was added to a solution of 0.50 g of **4** in 20 mL of chloroform. After the solution was stirred at room temperature for 20 min, all volatiles were removed in vacuum. Colorless crystals of the composition [**4**Me_2]$(CF_3SO_3)_2$·$CHCl_3$ were obtained from chloroform solution,

which was confirmed by X-ray structure analysis. However, in the absence of a solvent atmosphere, the crystals lose lattice-bound chloroform. Yield 83%. mp: 156−158 °C. ^{1}H NMR: 1.17−1.27 (m, 36H, CH_3), 1.94 (m, 6H, CH), 3.11 (m, 12H, CH_2), 4.29 (br, 6H, NH), 6.11 ppm (t, 6H, NCH_3, $^3J_{HP}$ = 9.6 Hz). ^{13}C{^{1}H} NMR: 25.9, 26.6, 33.4, 51.9 ppm. ^{31}P{^{1}H} NMR: 7.5 (d), 26.7 ppm (t, $^2J_{PP}$ = 30.7 Hz). IR ν(cm^{-1}): 3287 (N−H), 1294, 1286, 1118 (P−N_{ring}), 1103 (P−N_{ring}), 963, 932, 896, 812, 722. Anal. Calcd for $C_{45}H_{84}F_3N_9O_3P_3S$ (981.21): C, 55.08; H, 8.63; N, 12.85. Found C, 54.89; H, 8.23; N, 12.12%.

[7Me]I. Methyl iodide (1 mL) was added to a solution of 1.00 g of **7** in 20 mL of toluene. The solution was refluxed for 3 days. Colorless crystals of composition [**7**Me_2]I·MeI were obtained from toluene solution. The crystals lose lattice-bound methyl iodide in the absence of solvent atmosphere. Yield 79%. mp: 43−46 °C. ^{1}H NMR: 1.07−1.88 (m, 40H, CH_2), 2.95 (m, 4H, CH), 3.05 (t, 3H, NCH_3, $^3J_{HP}$ = 10.0 Hz), 4.28 ppm (br, 4H, NH). ^{13}C{^{1}H} NMR: 24.1, 24.4, 28.6, 34.2, 34.3, 50.7 ppm. ^{31}P{^{1}H} NMR: 12.0 (d), 17.3 ppm (t, $^2J_{PP}$ = 45.6 Hz). IR ν(cm^{-1}): 3321, 3134 (ν_s N−H), 1249, 1101 (ν_s P−N_{ring}), 1023 (ν_s P−N_{ring}), 1023, 867, 807, 722. Anal. Calcd for $C_{25}H_{51}Cl_2IN_9P_3$ (768.47): C, 39.07; H, 6.69; N, 16.40. Found C, 40.10; H, 6.55; N, 15.98%.

[8Me]I. Methyl iodide (1 mL) was added to a solution of 1.00 g of **8** in 20 mL of THF. The solution was refluxed for 3 days. Subsequently, all volatiles were removed in vacuum. Colorless crystals were obtained from slow evaporation of a methanol solution. Yield 80%. mp: 253−255 °C. ^{1}H NMR: 1.38 (s, 40H, CH_3), 3.08 (t, 3H, NCH_3, $^3J_{HP}$ = 9.8 Hz), 3.30 ppm (m, 4H, NH). ^{13}C{^{1}H} NMR: 31.1, 32.0, 54.5 ppm. ^{31}P{^{1}H} NMR: 7.7 (d), 13.6 ppm (t, $^2J_{PP}$ = 45.6 Hz). IR ν(cm^{-1}): 3230 (N−H), 3172 (N−H), 1250, 1229, 1195, 1070 (P−N_{ring}), 1032 (P−N_{ring}), 932, 869, 812, 737, 720, 630, 611. Anal. Calcd for $C_{17}H_{43}Cl_2IN_7P_3$ (636.29): C, 32.09; H, 6.81; N, 15.41. Found C, 32.45; H, 7.01; N, 15.65%.

[2Et]I. 2 (0.50 g) was dissolved in 10 mL of ethyl iodide. The mixture was stirred overnight at room temperature. Subsequently, excess ethyl iodide was removed under vacuum. Yield 89%. mp: 192−195 °C. ^{1}H NMR: 0.93 (m, 36H, CH_3), 1.35 (t, 3H, NCH_2−CH_3), 1.72 (m, 2H, CH), 1.82 (m, 4H, CH), 2.73 (m, 12H, CH_2), 3.55 (m, 2H, NCH_2-CH_3), 3.81 ppm (br, 6H, NH). ^{13}C{^{1}H} NMR: 15.3, 19.2, 28.7, 39.5, 47.7 ppm. ^{31}P{^{1}H} NMR: 14.2 (t), 16.9 ppm (d, $^2J_{PP}$ = 42.0 Hz). IR ν(cm^{-1}): 3223 (N−H), 1261, 119, 1171, 1093 (P−N_{ring}), 926 (P−N_{ring}), 825, 789, 755, 722. Anal. Calcd for $C_{26}H_{65}IN_9P_3$ (723.69): C, 43.15; H, 9.05; N, 17.42. Found C, 43.66; H, 9.22; N, 17.10%.

[2All]Br. 2 (1.00 g) was dissolved in 20 mL of toluene, and 0.5 mL (3 mol equiv) of allyl bromide was added. After the solution had been refluxed for 24 h, all volatiles were removed in vacuum. Colorless crystals were obtained from toluene solution. Yield 86%. mp: 135−137 °C. ^{1}H NMR: 0.86 (d, 36H, CH_3), 1.73 (m, 6H, CH), 2.66 (br, 12H, CH_2), 4.09 (br, 6H, NH), 5.12 (dd, 2H, CH=CH_2, $^3J_{HH(trans)}$ = 54.1 Hz, $^3J_{HH(cis)}$ = 47.9 Hz), 5.75 ppm (m, 1H, CH=CH_2). ^{13}C{^{1}H} NMR: 20.6, 30.1, 49.0, 117.6, 136.6 ppm. ^{31}P{^{1}H} NMR: 13.88 (t), 17.27 ppm (d, $^2J_{PP}$ = 47.17 Hz). IR ν(cm^{-1}): 3203 (N−H), 1641 (C=C), 1265, 1205, 1093 (P−N_{ring}), 1142 (P−N_{ring}), 982, 928, 856, 781, 766, 722. Anal. Calcd for $C_{27}H_{64}BrN_9P_3$ (687.69): C, 47.16; H, 9.38; N, 18.33. Found C, 46.94; H, 9.43; N, 17.80%.

[3All]Br. 3 (0.50 g) was dissolved in 20 mL of THF, and 0.38 mL (3 mol equiv) of allyl bromide was added. After the solution had been refluxed for 24 h, all volatiles were removed under vacuum. Colorless crystals were obtained from slow evaporation of a methanol solution. Yield 88%. mp: 179−182 °C. ^{1}H NMR: 1.06 (m, 36H, CH_3), 2.07 (m, 6H, CH), 3.93 (br, 6H, NH), 4.08 (m, 2H, NCH_2), 5.14 (dd, 2H, CH=CH_2, $^3J_{HH(trans)}$ = 54.5 Hz, $^3J_{HH(cis)}$ = 44.3 Hz), 5.55 ppm (m, 1H, CH=CH_2). ^{13}C{^{1}H} NMR: 24.4, 42.4, 48.2 ppm. ^{31}P{^{1}H} NMR: 9.39 (t), 11.12 ppm (d, $^2J_{PP}$ = 41.9 Hz). IR ν(cm^{-1}): 3192 (N−H), 1641 (C=C), 1365, 1303, 1269, 1223, 1168, 1142 (P−N_{ring}), 1038 (P−N_{ring}), 920, 887, 862, 818, 753, 722, 624, 605. Anal. Calcd for $C_{21}H_{53}BrN_9P_3$ (604.54): C, 41.79; H, 8.79; N, 20.90. Found C, 42.09; H, 8.91; N, 19.94%.

[6Bn]Br. 8 (0.50 g) was dissolved in 10 mL of THF, and 0.11 mL (1 mol equiv) of benzyl bromide was added. After the solution had been refluxed for 24 h, THF was removed under vacuum. Colorless crystals were obtained from a THF/hexane solution stored at −20 °C. Yield 86%. mp: −2 °C. ^{1}H NMR: 3.97 (m, 12H, CH_2,), 4.51 (br, 6H, NH), 4.72 (t, 2H, NCH_2−Ph, $^3J_{HP}$=11.4 Hz), 6.97−7.13 ppm (m, 35H, Ph). ^{13}C{^{1}H} NMR: 43.9, 48.5, 126.1, 127.4, 128.0 ppm. ^{31}P{^{1}H} NMR: 17.11 (t), 19.27 ppm (d, $^2J_{PP}$ = 44.6 Hz). IR ν(cm^{-1}): 3387 (N−H), 3171 (N−H), 1604, 1262, 1206,1096 (P−N_{ring}), 1071 (P−N_{ring}), 1027, 917, 873, 806, 772, 731, 697, 602. Anal. Calcd for $C_{42}H_{48}BrN_9P_3$ (942.86): C, 62.42; H, 5.88; N, 13.37. Found C, 63.13; H, 6.25; N, 13.35%.

Reactions of [2Me]I, [3Me]I, and [5Me]I with $AgNO_3$. Silver nitrate (0.10 g) was added to a methanol solution containing 0.20 g of *N*-methylphosphazenium iodide. The mixture was stirred for 1 h. The resulting silver iodide precipitate was removed by filtration. Colorless crystals were obtained from slow evaporation of a methanol solution. **Ag_2[2Me]$(NO_3)_3$·H_2O**: Yield 69%. ^{31}P{^{1}H} NMR (MeOH): 14.8 (t), 16.9 ppm (d, $^2J_{PP}$ = 43.2 Hz). Anal. Calcd for $C_{25}H_{65}Ag_2N_{12}O_{10}P_3$ (1002.53): C, 29.95; H, 6.53; N, 16.76. Found: C, 30.65; H, 6.12; N, 15.32%. **Ag[3Me]$(NO_3)_2$·MeOH**: Yield 62%. ^{31}P{^{1}H} NMR (MeOH): 9.03 (t), 12.45 ppm (d, $^2J_{PP}$ = 45.6 Hz). Anal. Calcd for $C_{19}H_{51}N_{11}P_3AgO_6$ (730.48): C, 31.24; H, 7.04; N, 21.09. Found C, 30.71; H, 7.01; N, 20.38%. **[5Me]-(NO_3)**: Yield 69%. ^{1}H NMR: 1.36 (s, 54H, CH_3), 2.99 (t, 3H, NCH_3), 3.74 ppm (br, 6H, NH). ^{13}C{^{1}H} NMR: 31.8, 52.3, 51.6 ppm. ^{31}P{^{1}H} NMR: 2.50 (t), 5.65 ppm (d, $^2J_{PP}$ = 42.6 Hz). IR ν(cm^{-1}): 3224 (N−H), 1332, 1266, 1228 (P−N_{ring}), 1178 (P−N_{ring}), 1064, 1042, 1028, 1014, 914, 887, 808, 722. Anal. Calcd for $C_{25}H_{63}N_{10}P_3O_3$ (644.43): C 42.57; H 8.85; N 17.72. Found C, 40.42; N, 8.42; H, 17.49%.

[3Ac]Cl. 3 (0.51 g) was dissolved in 20 mL of THF, and 0.08 mL (1 mol equiv) of freshly distilled acetyl chloride was added. After the solution had been stirred for 1 h, THF was removed under vacuum. Colorless crystals were obtained from a THF solution stored at 25 °C. Yield 68%. mp: 105−106 °C. ^{1}H NMR: 1.18 (m, 36H, CH_3), 1.94 (m, 6H, CH), 2.72 (s, 3H, COCH_3) 3.45 ppm (br, 6H, NH). ^{13}C{^{1}H} NMR: 24.8, 25.2, 43.6, 43.9 ppm. ^{31}P{^{1}H} NMR: 6.4 (t), 7.2 ppm (d, $^2J_{PP}$ = 39.7 Hz). IR ν(cm^{-1}): 3104 (N−H), 1672 (C=O), 1257, 1222, 1166 (P−N_{ring}), 1140 (P−N_{ring}), 1070, 1046, 975, 918, 860, 825, 763, 722, 632. Anal. Calcd for $C_{20}H_{51}ClN_9OP_3$ (562.06): C, 42.74; H, 9.15; N, 22.43. Found C, 42.43; H, 9.30; N, 21.69%.

[3Bz]Cl. 3 (0.76 g) was dissolved in 20 mL of THF, and 0.2 mL (1 mol equiv) of freshly distilled benzoyl chloride was added. After the solution had been stirred for 1 h, THF was removed under vacuum. Colorless crystals of the solvate [**3**Bz]Cl·$^1/_2$THF were obtained from a THF solution stored at 25 °C. Yield 65%. ^{1}H NMR: 1.19 (m, 36H, CH_3), 1.85 (m, 6H, CH), 3.44 (br, 6H, NH), 7.27−7.66 ppm (m, 5H, Ph). ^{13}C{^{1}H} NMR: 25.6, 25.9, 43.7, 44.5 ppm. ^{31}P{^{1}H} NMR: 8.7 (t), 9.8 ppm (d, $^2J_{PP}$ = 35.5 Hz). IR ν(cm^{-1}): 3202 (N−H), 1771, 1634 (C=O), 1283, 1167 (P−N_{ring}), 1115 (P−N_{ring}), 1037, 971, 857, 805, 756, 720, 688. Anal. Calcd

for $C_{25}H_{53}N_9P_3ClO$ (624.13): C, 48.11; H, 8.56; N, 20.20. Found C, 47.77; N, 8.66; H, 19.96%.

9. 3 (0.35 g) was dissolved in 15 mL of THF, and 0.10 g of bromoacetic acid was added. The reaction mixture was refluxed overnight. All volatiles were removed under vacuum. Colorless crystals of **9** were obtained from a THF/hexane solution among a white precipitate containing [**3**H]$^+$ ions. $^{31}P\{^1H\}$ NMR: 6.2 (dd, $^2J_{PP}$ = 29.6, 41.3 Hz), 9.5 (s, [**3**H]$^+$), 9.8 (dd, $^2J_{PP}$ = 41.3, 46.5 Hz), 19.7 ppm (dd, $^2J_{PP}$ = 29.5, 46.5 Hz).

X-ray Crystallography. Crystallographic data were recorded on a Bruker Smart Apex diffractometer using Mo Kα radiation (λ = 0.71073 Å) at T = 100 K (data of [**2**Et]I and [**6**Bn]Br•2THF were recorded on a Stoe IPDS diffractometer using Mo Kα radiation at T = 200 K). Empirical absorption corrections were applied (SADABS). Structures were solved by direct methods and refined by full-matrix least-squares against F^2 using all data (SHELXTL).[17] Unless otherwise stated, all non-hydrogen atoms were refined anisotropically with the exception of disordered atoms. H atoms were fixed in calculated positions at parent atoms. H atoms of NH units and those of hydrogen-bonded solvent molecules were refined freely using similar distance restraints for N−H bonds. Disordered atoms were split on two positions and refined using similar distance and similar U restraints. Data of [**1**Me]I were truncated at 2θ = 35°, and all atoms except iodine were refined isotropically due the low resolution of the very weakly diffracting crystals. [**5**Me]I and [**5**Me](NO_3) were refined as non-merohedral twins exhibiting batch scale factors of 0.386 and 0.536, respectively.

(17) Sheldrick, G. M. *SHELX97, Programme for X-ray crystal structure solution and refinement*; Universität Göttingen: Göttingen, Germany, 1997.

Acknowledgment. We thank the EPSRC for financial support.

Supporting Information Available: X-ray crystallographic data in CIF format. This material is available free of charge via the Internet at http://pubs.acs.org.

IC7009463